Electronic Supplementary Information on

A step closer to the binary: The $^{1}_{\infty}[Bi_6I_{20}]^{2-}$ anion

Johanna Heine

Fachbereich Chemie and Wissenschaftliches Zentrum für Materialwissenschaften (WZMW),

Philipps-Universität Marburg, Hans-Meerwein-Straße, 35043 Marburg, Germany

Crystallographic details

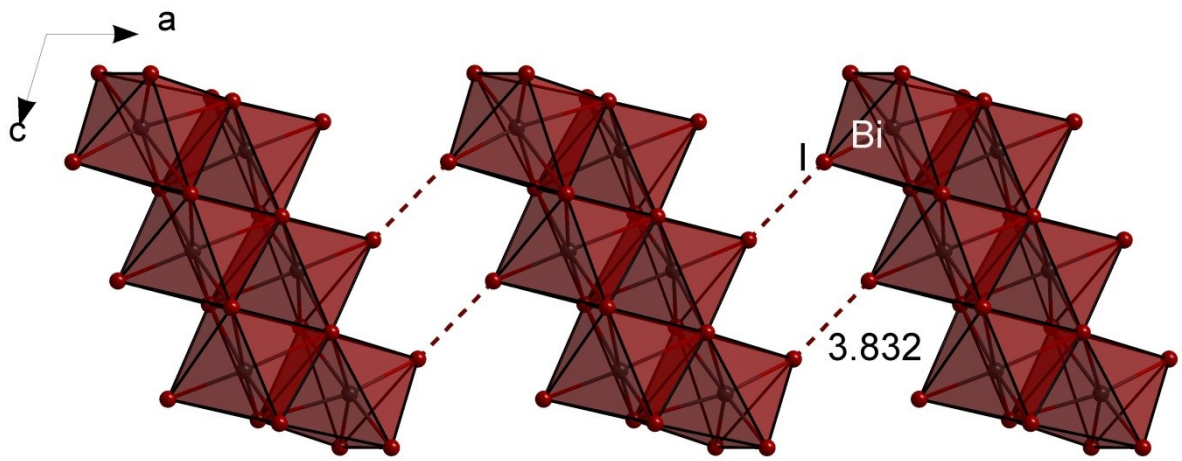

Figure S1. I…I-interaction in **1**. BiI_6 units are shown as dark red polyhedra, Bi atoms in dark grey and I atoms in dark red. Dashed lines show the I…I interaction with an interatomic distance of 3.832 Å.

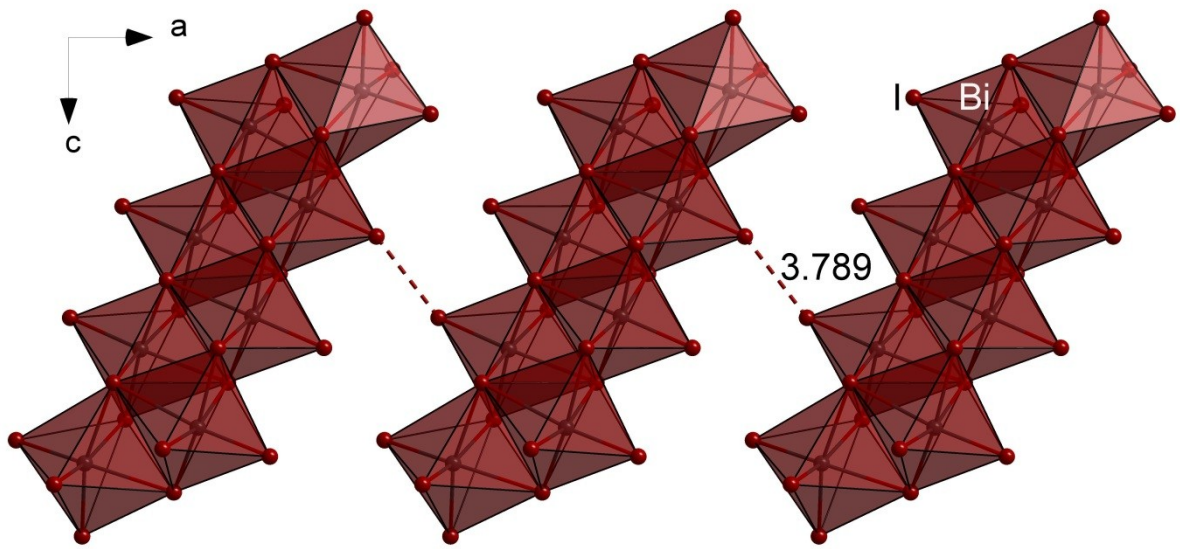

Figure S2. I…I-interaction in **2**. BiI_6 units are shown as dark red polyhedra, Bi atoms in dark grey and I atoms in dark red. Dashed lines show the I…I interaction with an interatomic distance of 3.789 Å.

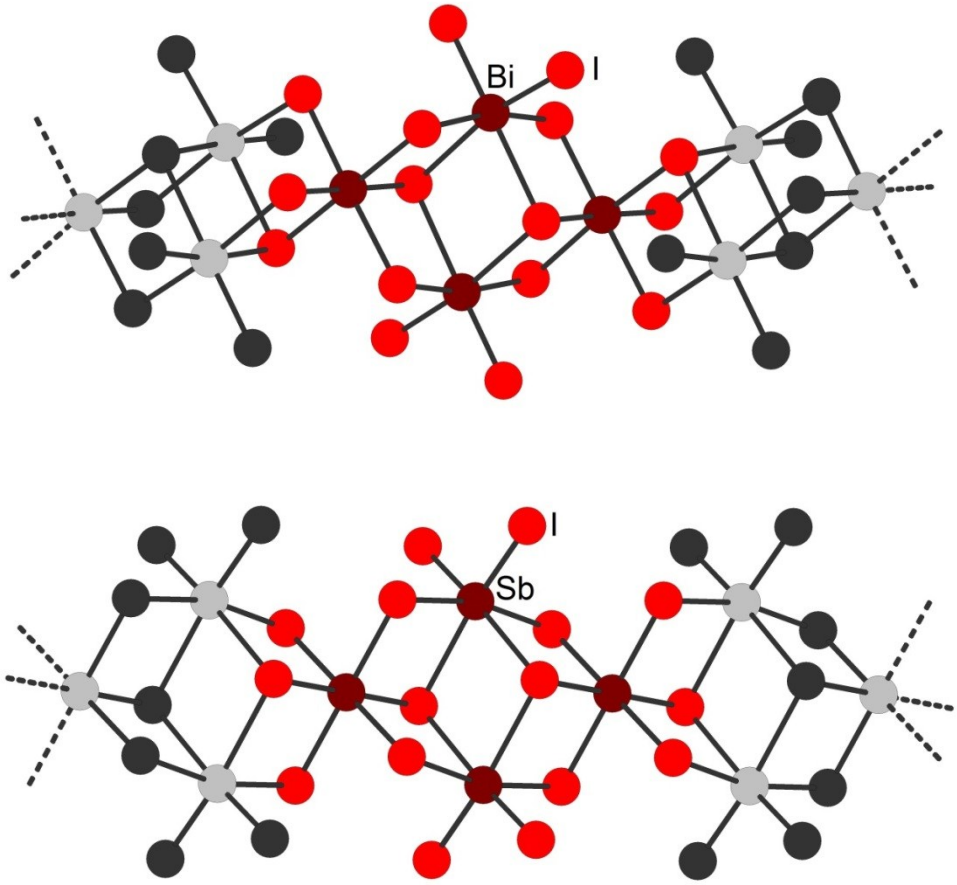

Figure S3. Direct comparison of the anionic strands in **3** (top) and $[PPh_4][Sb_3I_{10}]$ (bottom). Pentel atoms are depicted in light grey, I atoms in dark grey. A $[Bi_4I_{16}]$ unit has been highlighted in red in both anionic substructures.

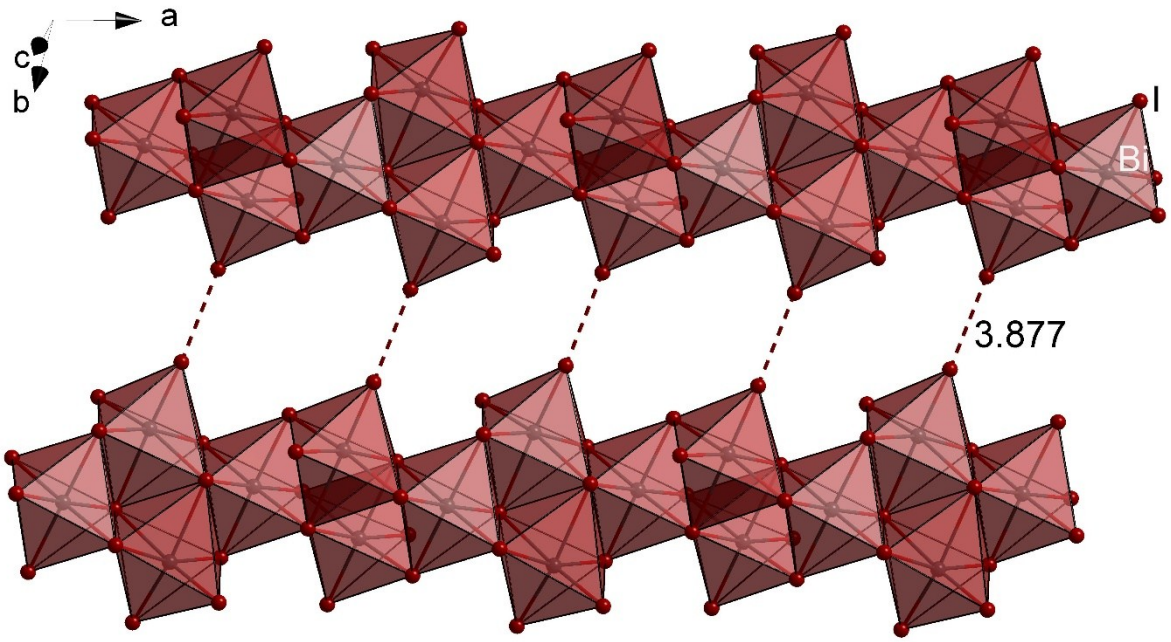

Figure S4. I…I-interaction in **3**. BiI_6 units are shown as dark red polyhedra, Bi atoms in dark grey and I atoms in dark red. Dashed lines show the I…I interaction with an interatomic distance of 3.877 Å.

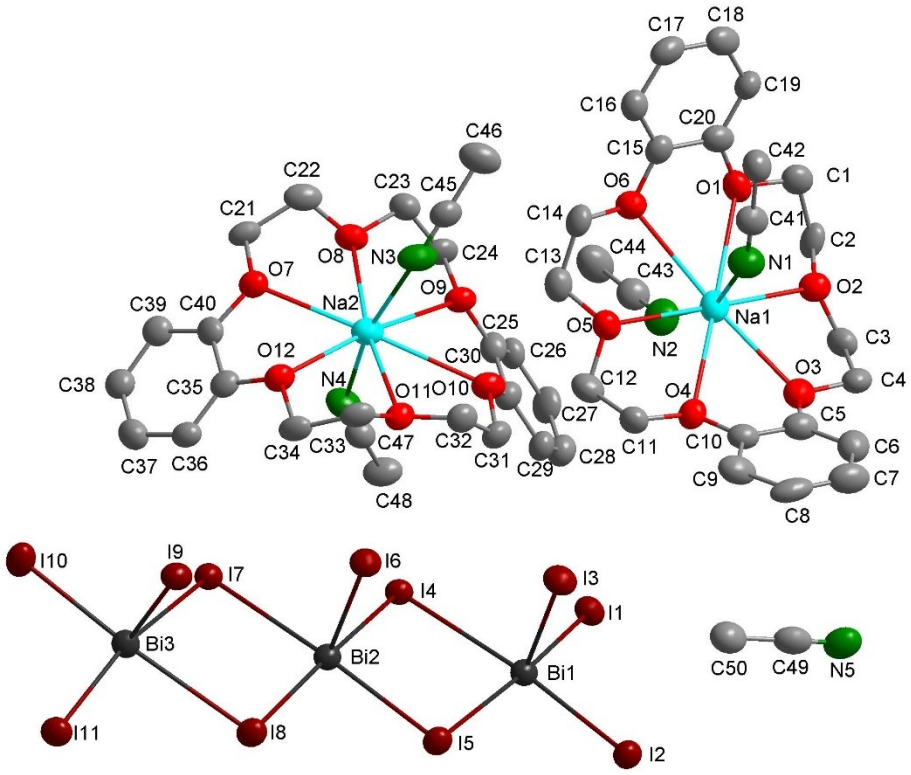

Figure S5: Asymmetric unit of **1**, ellipsoids at 50% probability.

Table S1: Selected interatomic distances (in A) and angles (in °) in **1**.

Symmetry operation: I 1-x, 1-y, 2-z

Bi1 I1	2.9531(8)	Na2 N4	2.374(11)	I2 Bi1 I7^{I}	87.90(2)
Bi1 I3	2.8893(9)	Na1 O5	2.512(9)	I2 Bi1 I4	174.56(3)
Bi1 I5	3.2670(9)	Na1 O6	2.837(9)	I11 Bi3 I8	92.02(2)
Bi1 I7^{I}	3.3669(8)	Na1 O2	2.521(9)	I11 Bi3 I10	93.50(3)
Bi1 I4	3.2797(9)	Na1 O4	2.673(8)	I9 Bi3 I11	96.36(2)
Bi1 I2	2.9116(9)	Na1 O1	2.802(9)	I9 Bi3 I8	87.96(2)
Bi3 I11	2.8824(9)	Na1 O3	2.633(10)	I9 Bi3 I10	93.18(3)
Bi3 I8	3.3291(10)	Na1 N1	2.403(10)	I10 Bi3 I8	174.21(2)
Bi3 I9	2.8695(8)	Na1 N2	2.466(10)	I6 Bi2 I5	95.71(2)
Bi3 I10	2.9190(10)			I6 Bi2 I7	89.46(2)
Bi2 I6	2.8577(8)	I1 Bi1 I5	173.44(2)	I6 Bi2 I4^{I}	176.93(2)
Bi2 I5	3.0270(9)	I1 Bi1 I7^{I}	87.68(2)	I6 Bi2 I4	91.95(2)
Bi2 I7	3.1860(9)	I1 Bi1 I4	90.25(2)	I6 Bi2 I8	97.96(2)
Bi2 I4	3.2007(8)	I3 Bi1 I1	93.83(2)	I5 Bi2 I7	174.71(2)
Bi2 I4^{I}	3.3778(8)	I3 Bi1 I5	90.22(2)	I5 Bi2 I4	90.04(2)
Bi2 I8	2.9888(9)	I3 Bi1 I7^{I}	177.23(3)	I5 Bi2 I4^{I}	85.23(2)
Na2 O7	2.666(9)	I3 Bi1 I4	89.49(2)	I7 Bi2 I4^{I}	89.55(2)
Na2 O11	2.579(7)	I3 Bi1 I2	94.32(3)	I7 Bi2 I4	88.66(2)
Na2 O9	2.782(9)	I5 Bi1 I7^{I}	88.07(2)	I4 Bi2 I4^{I}	85.12(2)
Na2 O12	2.545(9)	I5 Bi1 I4	84.62(2)	I8 Bi2 I5	90.27(2)
Na2 O8	2.536(8)	I4 Bi1 I7^{I}	88.178(19)	I8 Bi2 I7	90.13(2)
Na2 O10	2.868(10)	I2 Bi1 I1	93.35(3)	I8 Bi2 I4^{I}	84.95(2)
Na2 N3	2.436(11)	I2 Bi1 I5	91.48(2)	I8 Bi2 I4	170.00(2)

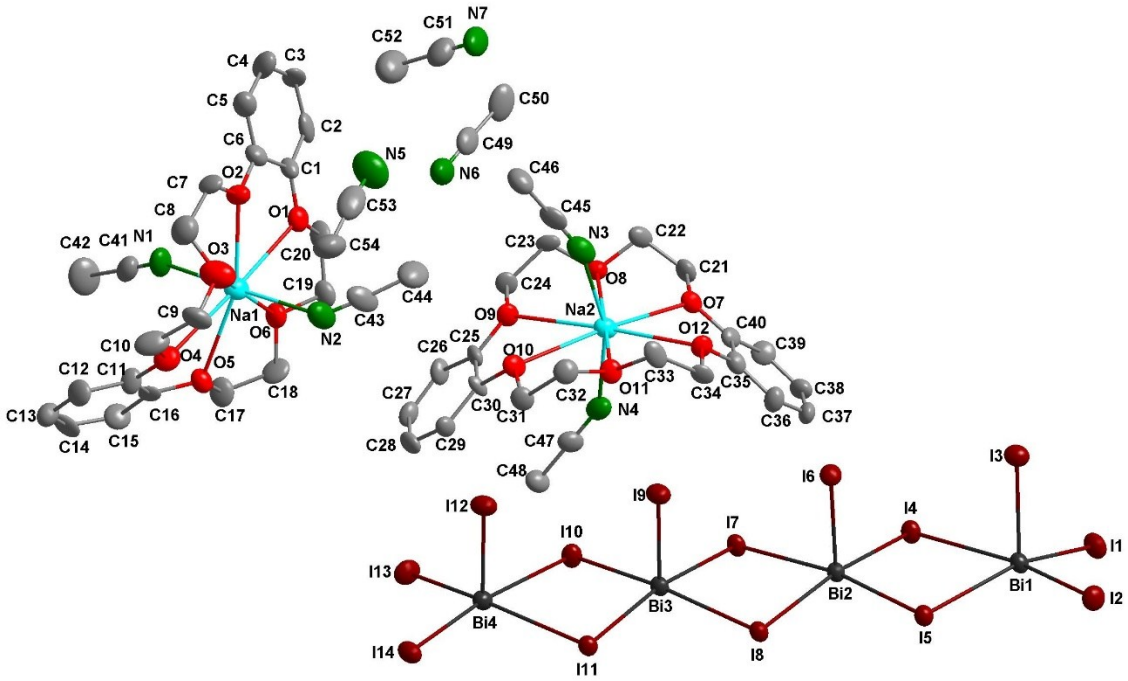

Figure S6: Asymmetric unit of **2**, ellipsoids at 50% probability.

Table S2: Selected interatomic distances (in A) and angles (in °) in **2**.

Symmetry operation: I -x, 1-y, 1-z

Bi2 I11^{I}	3.4261(13)	Na1 O2	2.519(14)	I10 Bi3 I11	93.99(3)
Bi2 I8	3.1895(13)	Na1 O5	2.732(14)	I10 Bi3 I8	171.43(4)
Bi2 I5	3.0512(12)	Na1 O1	2.683(15)	I10 Bi3 I8^{I}	85.64(3)
Bi2 I4	2.9876(13)	Na1 O6	2.509(14)	I10 Bi3 I7	89.33(3)
Bi2 I7	3.1526(11)	Na1 O4	2.827(16)	I9 Bi3 I11	92.21(4)
Bi2 I6	2.8508(13)	Na1 O3	2.518(16)	I9 Bi3 I8^{I}	177.19(4)
Bi3 I11	3.1312(13)	Na1 N1	2.429(16)	I9 Bi3 I8	91.89(4)
Bi3 I8	3.2238(12)	Na1 N2	2.468(18)	I9 Bi3 I7	96.16(4)
Bi3 I8^{I}	3.4068(13)			I9 Bi3 I10	96.27(4)
Bi3 I7	3.0712(13)	I8 Bi2 I11^{I}	84.39(3)	I10 Bi4 I11	83.39(3)
Bi3 I10	2.9709(12)	I5 Bi2 I11^{I}	90.56(3)	I14 Bi4 I11	92.65(4)
Bi3 I9	2.8445(13)	I5 Bi2 I8	86.06(3)	I14 Bi4 I10	172.90(4)
Bi4 I11	3.3903(12)	I5 Bi2 I7	170.42(4)	I12 Bi4 I11	91.41(3)
Bi4 I10	3.3201(14)	I4 Bi2 I11^{I}	87.34(3)	I12 Bi4 I10	92.02(4)
Bi4 I14	2.9278(14)	I4 Bi2 I8	171.51(4)	I12 Bi4 I14	93.98(4)
Bi4 I12	2.8482(13)	I4 Bi2 I5	92.12(3)	I12 Bi4 I13	98.92(4)
Bi4 I13	2.8573(13)	I4 Bi2 I7	94.45(3)	I13 Bi4 I11	165.91(4)
Bi1 I5	3.4240(13)	I7 Bi2 I11^{I}	82.80(3)	I13 Bi4 I10	86.69(4)
Bi1 I4	3.4070(12)	I7 Bi2 I8	86.42(3)	I13 Bi4 I14	96.13(4)
Bi1 I2	2.8878(12)	I6 Bi2 I11^{I}	174.82(4)	I4 Bi1 I5	79.08(3)
Bi1 I3	2.8702(14)	I6 Bi2 I8	94.91(4)	I2 Bi1 I5	87.50(4)
Bi1 I1	2.8566(13)	I6 Bi2 I5	94.52(3)	I2 Bi1 I4	166.53(4)
Na2 O9	2.760(12)	I6 Bi2 I4	93.51(4)	I3 Bi1 I5	101.22(4)
Na2 O7	2.615(13)	I6 Bi2 I7	92.03(4)	I3 Bi1 I4	84.96(3)
Na2 O10	2.750(14)	I11 Bi3 I8	88.28(3)	I3 Bi1 I2	96.70(4)
Na2 O12	2.700(12)	I11 Bi3 I8^{I}	85.60(3)	I1 Bi1 I5	163.77(4)
Na2 O8	2.597(12)	I8 Bi3 I8^{I}	86.29(3)	I1 Bi1 I4	98.26(3)
Na2 O11	2.521(12)	I7 Bi3 I11	170.60(4)	I1 Bi1 I2	94.94(4)
Na2 N3	2.47(2)	I7 Bi3 I8^{I}	85.89(3)	I1 Bi1 I3	94.45(4)
Na2 N4	2.414(18)	I7 Bi3 I8	87.20(3)		

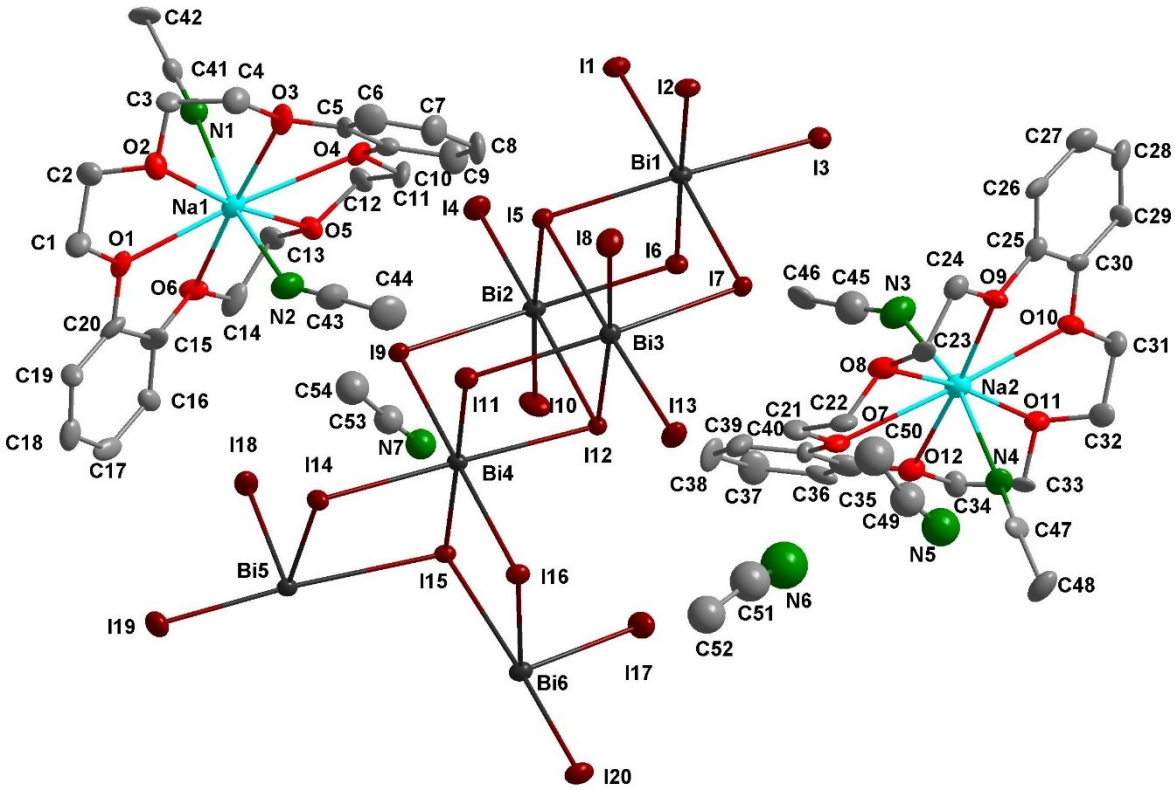

Figure S7: Asymmetric unit of **3**, ellipsoids at 50% probability.

Table S3: Selected interatomic distances (in A) and angles (in °) in **3**.

Symmetry operation: I 1-x, -y, -z

Bi1 I7	3.0956(16)	I2 Bi1 I7	88.76(4)	I7 Bi3 I12	86.39(4)
Bi1 I5	3.0641(17)	I2 Bi1 I5	89.71(4)	I7 Bi3 I5	85.40(4)
Bi1 I2	3.0230(16)	I2 Bi1 I1	91.85(4)	I7 Bi3 I11	169.16(5)
Bi1 I1	3.0468(16)	I2 Bi1 I6	178.91(5)	I5 Bi3 I12	82.64(4)
Bi1 I6	3.0972(17)	I2 Bi1 I3	93.38(5)	I11 Bi3 I12	85.69(4)
Bi1 I3	3.0756(17)	I1 Bi1 I7	178.47(5)	I11 Bi3 I5	86.25(4)
Bi4 I16	3.1042(16)	I1 Bi1 I5	87.71(4)	I13 Bi3 I7	91.22(5)
Bi4 I15	3.0525(16)	I1 Bi1 I6	88.76(5)	I13 Bi3 I12	94.03(5)
Bi4 I12	3.0734(16)	I1 Bi1 I3	93.11(5)	I13 Bi3 I5	175.39(5)
Bi4 I9	3.0523(16)	I3 Bi1 I7	88.25(4)	I13 Bi3 I11	96.71(5)
Bi4 I11	3.0775(17)	I3 Bi1 I6	85.69(4)	I8 Bi3 I7	94.06(5)
Bi4 I14	3.0877(17)	I15 Bi4 I16	90.15(4)	I8 Bi3 I12	171.24(5)
Bi6 I16	3.0620(17)	I15 Bi4 I12	90.45(4)	I8 Bi3 I5	88.67(5)
Bi6 I15	3.3521(16)	I15 Bi4 I11	175.62(5)	I8 Bi3 I11	92.65(5)
Bi6 I2^{I}	3.4126(17)	I15 Bi4 I14	90.15(4)	I8 Bi3 I13	94.71(6)
Bi6 I3^{I}	3.1062(17)	I12 Bi4 I16	87.43(4)	I1^{I} Bi5 I15	85.18(4)
Bi6 I20	2.8824(16)	I12 Bi4 I11	92.15(4)	I1^{I} Bi5 I14	164.91(5)
Bi6 I17	2.8262(18)	I12 Bi4 I14	178.48(5)	I14 Bi5 I15	83.55(4)
Bi3 I7	3.0860(16)	I9 Bi4 I16	178.95(5)	I18 Bi5 I15	89.00(5)
Bi3 I12	3.3801(17)	I9 Bi4 I15	88.99(4)	I18 Bi5 I1^{I}	94.03(5)
Bi3 I5	3.3790(16)	I9 Bi4 I12	91.96(4)	I18 Bi5 I14	95.79(5)
Bi3 I11	3.1291(17)	I9 Bi4 I11	94.44(5)	I18 Bi5 I19	94.88(5)
Bi3 I13	2.8741(16)	I9 Bi4 I14	89.44(4)	I19 Bi5 I15	176.02(5)
Bi3 I8	2.8186(18)	I11 Bi4 I16	86.45(4)	I19 Bi5 I1^{I}	93.66(5)
Bi5 I15	3.4003(16)	I11 Bi4 I14	87.16(4)	I19 Bi5 I14	96.90(5)
Bi5 I1^{I}	3.0808(17)	I14 Bi4 I16	91.17(4)	I12 Bi2 I5	82.33(4)
Bi5 I14	3.1178(17)	I16 Bi6 I15	85.51(4)	I9 Bi2 I12	84.89(4)
Bi5 I18	2.8344(16)	I16 Bi6 I2^{I}	85.95(4)	I9 Bi2 I5	83.65(4)
Bi5 I19	2.8708(17)	I16 Bi6 I3^{I}	168.36(5)	I6 Bi2 I12	86.75(4)
Bi2 I12	3.3897(16)	I15 Bi6 I2^{I}	82.06(4)	I6 Bi2 I5	85.53(4)
Bi2 I5	3.3906(16)	I3^{I} Bi6 I15	85.35(4)	I6 Bi2 I9	167.11(5)
Bi2 I9	3.1319(16)	I3^{I} Bi6 I2^{I}	85.67(4)	I4 Bi2 I12	177.26(5)
Bi2 I6	3.0854(17)	I20 Bi6 I16	93.21(5)	I4 Bi2 I5	95.58(5)
Bi2 I4	2.8581(16)	I20 Bi6 I15	176.63(5)	I4 Bi2 I9	93.14(5)
Bi2 I10	2.8257(17)	I20 Bi6 I2^{I}	94.75(5)	I4 Bi2 I6	94.86(5)
		I20 Bi6 I3^{I}	95.52(5)	I10 Bi2 I12	86.59(5)
		I17 Bi6 I16	94.31(5)	I10 Bi2 I5	168.88(5)
I7 Bi1 I6	90.65(4)	I17 Bi6 I15	88.43(5)	I10 Bi2 I9	94.39(5)
I5 Bi1 I7	90.90(4)	I17 Bi6 I2^{I}	170.44(5)	I10 Bi2 I6	94.88(5)
I5 Bi1 I6	91.22(4)	I17 Bi6 I3^{I}	92.62(5)	I10 Bi2 I4	95.46(5)
I5 Bi1 I3	176.78(5)	I17 Bi6 I20	94.78(6)		

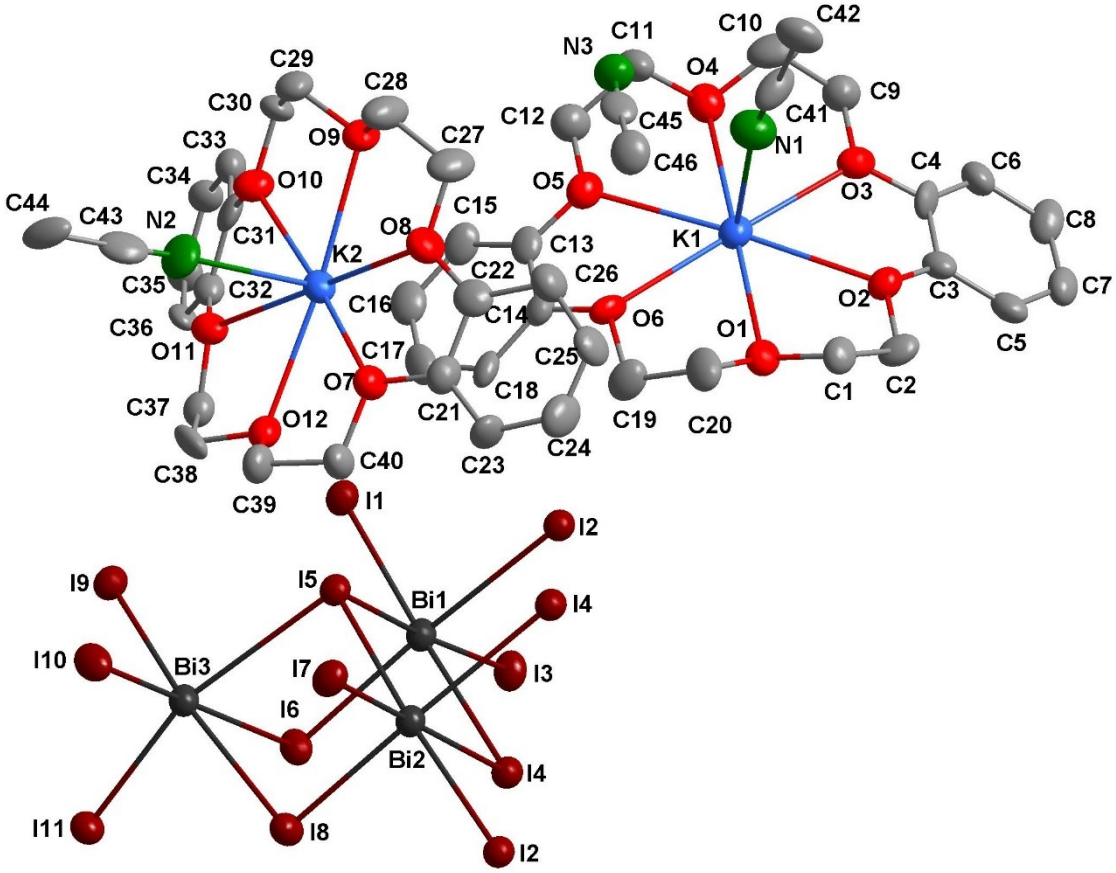

Figure S8: Asymmetric unit of **4**, ellipsoids at 50% probability.

Table S4: Selected interatomic distances (in A) and angles (in °) in **4**.

Symmetry operations: I 2-x, 1-y, -z

Bi1 I4	3.3247(11)	K2 N2	2.811(15)	$I2^{I}$ Bi2 I4	84.53(3)
Bi1 I2	3.2269(11)	K1 O6	2.826(11)	$I2^{I}$ Bi2 $I4^{I}$	90.84(3)
Bi1 I5	3.3434(10)	K1 O4	2.781(12)	$I2^{I}$ Bi2 I5	171.39(3)
Bi1 I1	2.9122(11)	K1 O2	2.740(10)	I5 Bi2 I4	86.95(3)
Bi1 I3	2.8939(10)	K1 O5	2.732(11)	I5 Bi2 $I4^{I}$	87.36(3)
Bi1 I6	2.9757(11)	K1 O3	2.727(11)	I7 Bi2 $I4^{I}$	93.31(3)
Bi2 $I4^{I}$	3.2011(11)	K1 O1	2.699(11)	I7 Bi2 I4	179.10(3)
Bi2 I4	3.3866(10)	K1 N1	2.788(15)	I7 Bi2 $I2^{I}$	94.64(3)
Bi2 $I2^{I}$	3.0155(11)	K1 C11	3.516(13)	I7 Bi2 I5	93.87(3)
Bi2 I5	3.1199(11)	K1 C1	3.509(12)	I7 Bi2 I8	93.38(3)
Bi2 I7	2.8879(11)	K1 $C7^{II}$	3.390(16)	I8 Bi2 I4	87.00(3)
Bi2 I8	2.9772(11)	K1 $C8^{II}$	3.146(15)	I8 Bi2 $I4^{I}$	172.92(3)
Bi3 I5	3.3503(11)			I8 Bi2 $I2^{I}$	90.92(3)
Bi3 I6	3.4016(10)	I4 Bi1 I5	84.44(2)	I8 Bi2 I5	89.89(3)
Bi3 I8	3.3077(11)	I2 Bi1 I4	85.07(3)	I5 Bi3 I6	83.73(2)
Bi3 I9	2.9053(11)	I2 Bi1 I5	84.74(3)	I8 Bi3 I5	80.64(3)
Bi3 I11	2.8907(11)	I1 Bi1 I4	167.53(3)	I8 Bi3 I6	86.20(3)
Bi3 I10	2.8767(10)	I1 Bi1 I2	88.88(3)	I9 Bi3 I5	94.87(3)
I4 $Bi2^{I}$	3.2010(11)	I1 Bi1 I5	84.15(3)	I9 Bi3 I6	88.28(3)
I2 $Bi2^{I}$	3.0154(11)	I1 Bi1 I6	96.72(3)	I9 Bi3 I8	173.23(3)
K2 O7	2.765(11)	I3 Bi1 I4	92.66(3)	I11 Bi3 I5	163.86(3)
K2 O12	2.695(10)	I3 Bi1 I2	90.06(3)	I11 Bi3 I6	85.45(3)
K2 O11	2.816(11)	I3 Bi1 I5	174.24(3)	I11 Bi3 I8	86.73(3)
K2 O10	2.763(11)	I3 Bi1 I1	98.26(3)	I11 Bi3 I9	96.74(3)
K2 O9	2.718(10)	I3 Bi1 I6	94.12(3)	I10 Bi3 I5	95.13(3)
K2 O8	2.745(11)	I6 Bi1 I4	88.46(3)	I10 Bi3 I6	178.17(4)
K2 C16	3.479(15)	I6 Bi1 I2	172.46(3)	I10 Bi3 I8	92.20(3)
K2 C29	3.504(12)	I6 Bi1 I5	90.78(3)	I10 Bi3 I9	93.25(3)
K2 C17	3.167(14)	$I4^{I}$ Bi2 I4	86.34(3)	I10 Bi3 I11	95.37(3)

Thermal analysis

The thermal behavior of **1** (8.7 mg), **2** (7.6 mg), **3** (15.0 mg) and **4** (7.5 mg) was studied by simultaneous DTA/TG on a *NETZSCH STA 409 C/CD* in from 25 °C to 800 °C with a heating rate of 10 °C min^{-1} in a constant flow of 80 ml min^{-1} Ar. For all four compounds, TG data (residual masses of less than 10%) and DSC data (DSC peaks at the corresponding melting points) suggest that the final material is composed of NaI for **1**-**3** and KI for **4**.

1: The first, two-step mass loss of 6% corresponds to the loss of nine molecules of MeCN per formula unit. Thus, isolated **1** has formula of $[(DB18C6)Na(MeCN)_2]_4[Bi_6I_{22}]\cdot 1$ MeCN. The loss of solvate is possibly aggravated by evacuating the furnace chamber prior to the measurement. Two endothermic peaks can be observed during a TG trace plateau between 200 and 350°C, indicating melting and an additional phase transition. At 350°C a complex exothermic decomposition step sets in.

2: The first, two-step mass loss of 8% corresponds to the loss of 14 molecules of MeCN per formula unit. Thus, **2** retains the original formula of $[(DB18C6)Na(MeCN)_2]_4[Bi_8I_{28}]\cdot 6$ MeCN, at least shortly after isolation from the mother liquor. One broad endothermic peak can be observed during a TG trace plateau between 200 and 350°C, indicating melting and possibly an additional phase transition. At 350°C a complex exothermic decomposition step sets in.

3: The first mass loss of 3% corresponds to the loss of 3.5 molecules of MeCN per formula unit. Thus, isolated **3** has formula of $[(DB18C6)Na(MeCN)_2]_2[Bi_6I_{20}]$ with an additional partial loss of coordinating MeCN molecules. This observation corresponds to the difficulty experienced in isolating a non-fractured crystal for SCXRD measurements. One endothermic peak can be observed during a TG trace plateau between 200 and 350°C, indicating melting or another phase transition. At 350°C a complex exothermic decomposition step sets in.

4: The first mass loss of 2% corresponds to the loss of 3 molecules of MeCN per formula unit. Thus, isolated **4** has formula of $[(DB18C6)K(MeCN)]_4[Bi_6I_{22}]$ with an additional partial loss of coordinating MeCN molecules. One endothermic peak can be observed during a TG trace plateau between 200 and 350°C, indicating melting or another phase transition. At 350°C a complex exothermic decomposition step sets in.

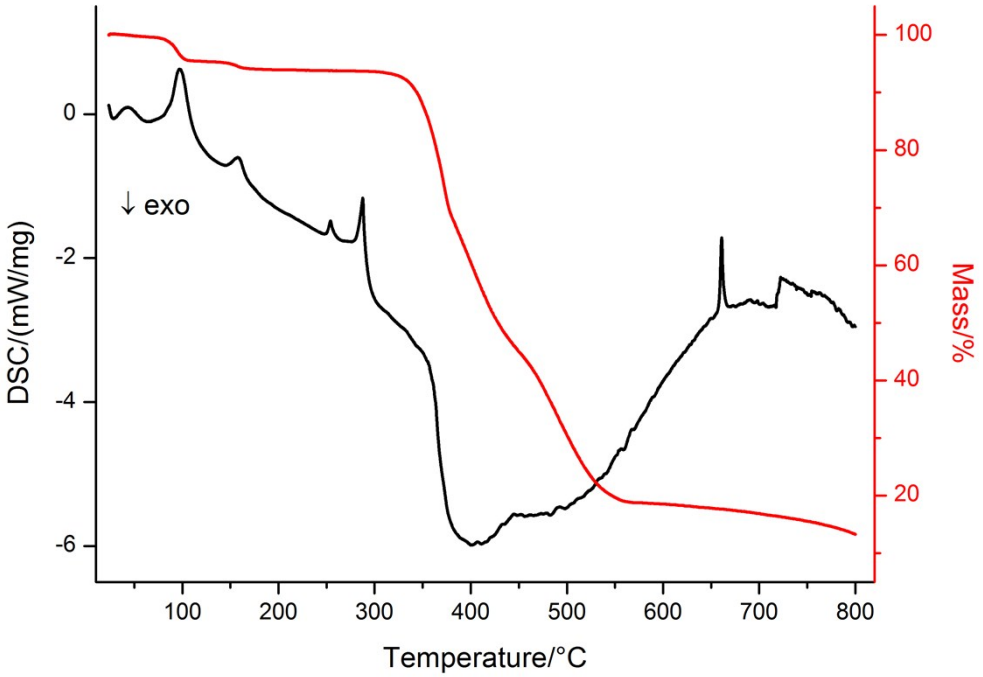

Figure S9. Simultaneous DTA/TG of **1**.

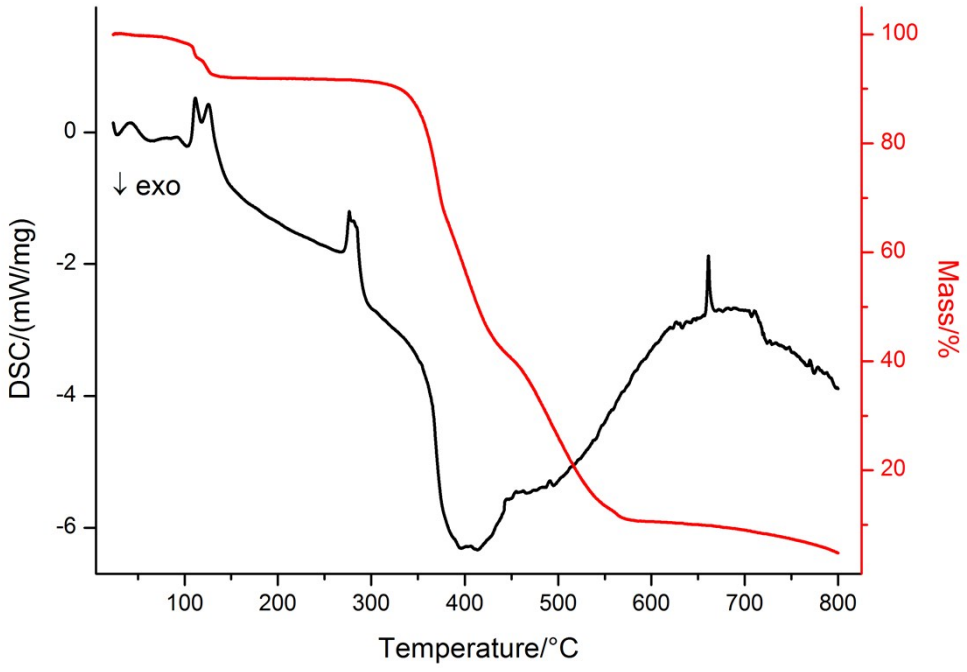

Figure S10. Simultaneous DTA/TG of **2**.

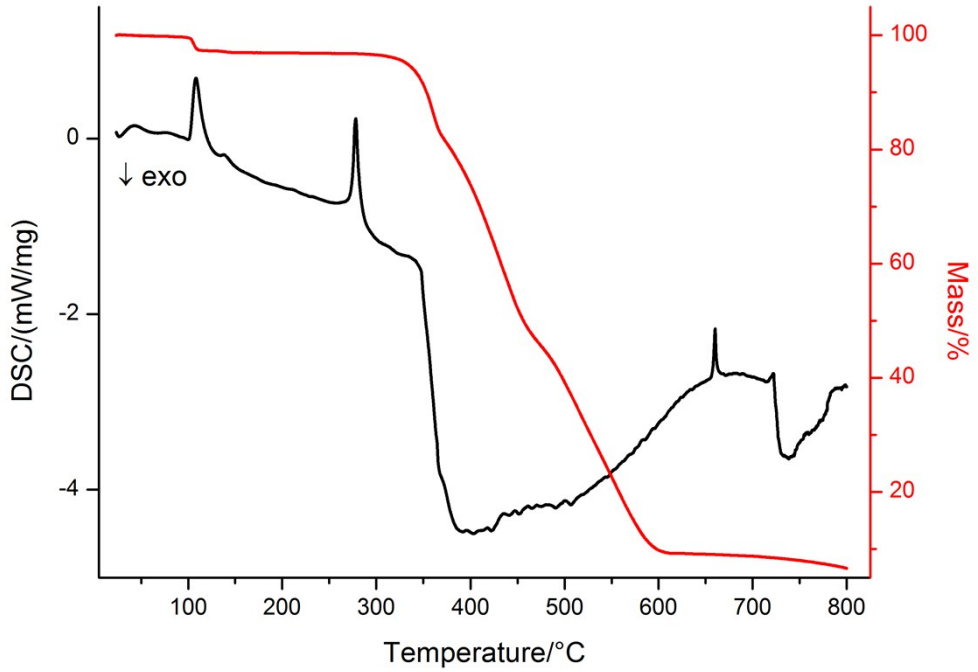

Figure S11. Simultaneous DTA/TG of **3**.

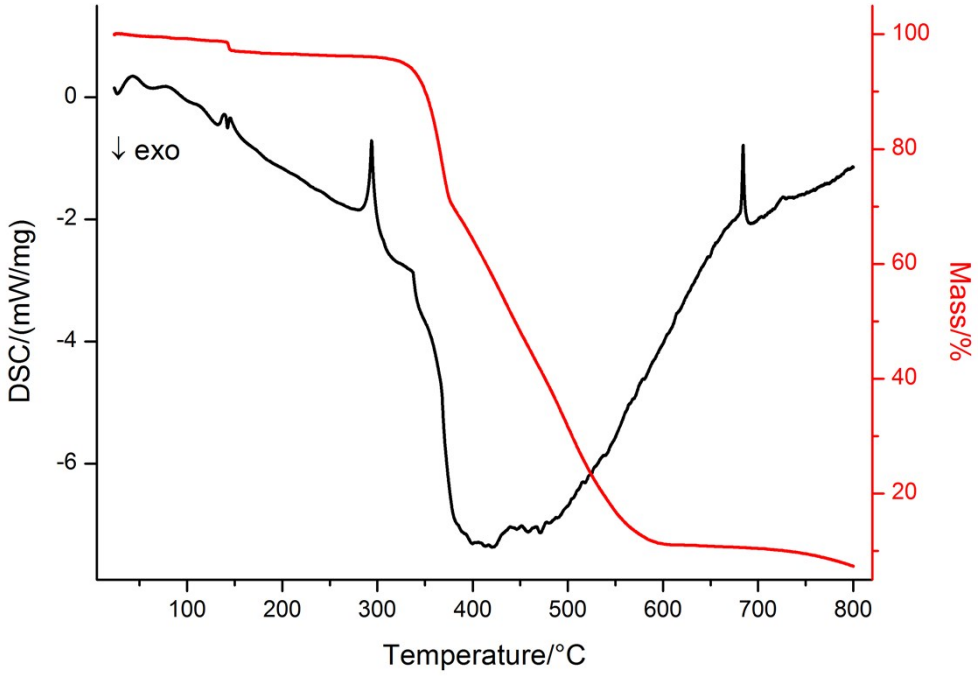

Figure S12. Simultaneous DTA/TG of **4**.

Powder diffraction

Powder patterns of **1**-**4** were recorded on a Panalytical X'Pert Pro PW3040/60 with $CuK_{\alpha 1}$ radiation with λ= 1.54056 Å or on a Panalytical X'Pert Pro with CuK_{α} radiation with λ= 1.54 Å at room temperature. The patterns confirm the presence of the phase determined by the respective SCXRD measurements and also indicate a partial degradation of crystallinity upon desolvation.

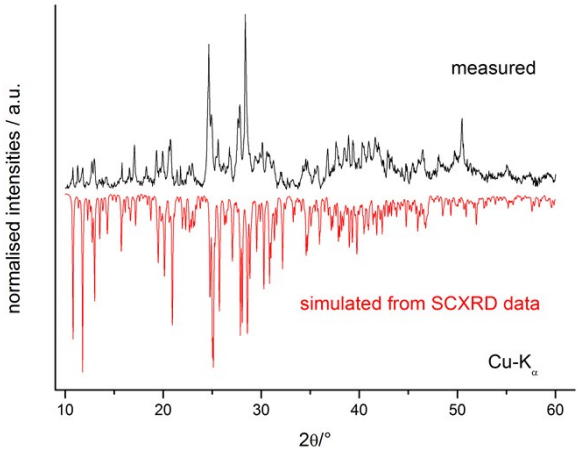

Figure S13. Powder diffraction pattern of compound **1**

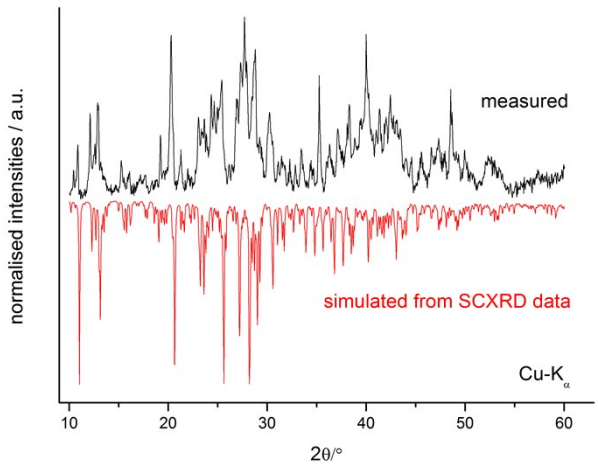

Figure S14. Powder diffraction pattern of compound **2**

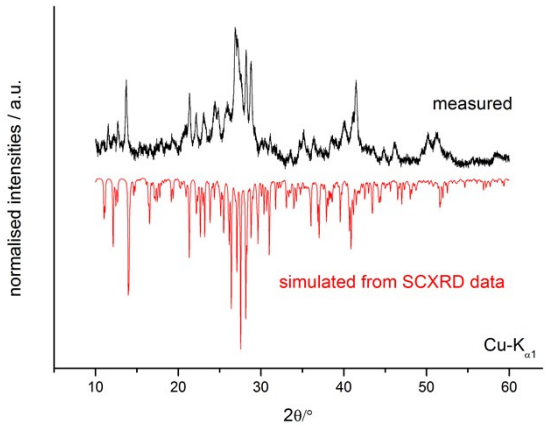

Figure S15. Powder diffraction pattern of compound **3**

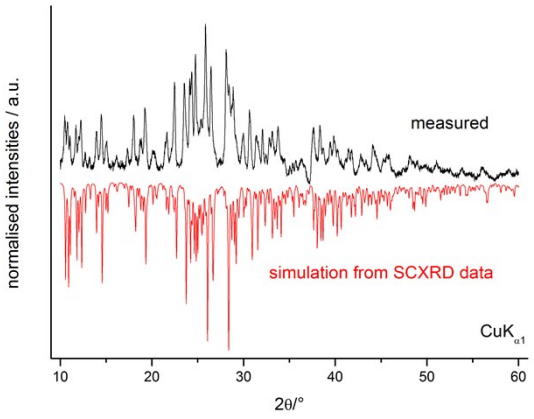

Figure S16. Powder diffraction pattern of compound **4**

IR spectra

IR spectra of **1**-**4** were recorded on a *Bruker Tensor 37* FT-IR spectrometer equipped with an ATR-Platinum measuring unit. All spectra are similar in appearance with the MIR region dominated by bands of the $[(DB18C6)A(MeCN)_n]^+$ cations.

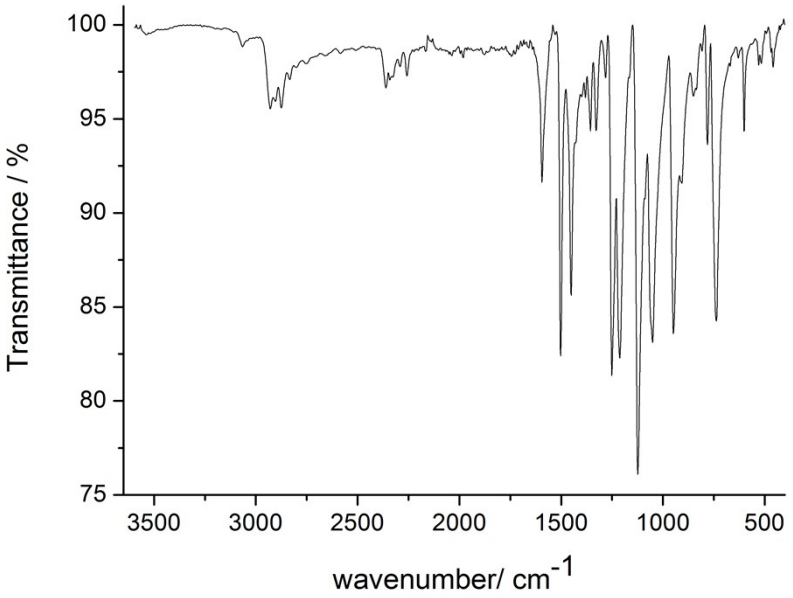

Figure S17. IR spectrum of compound **1**

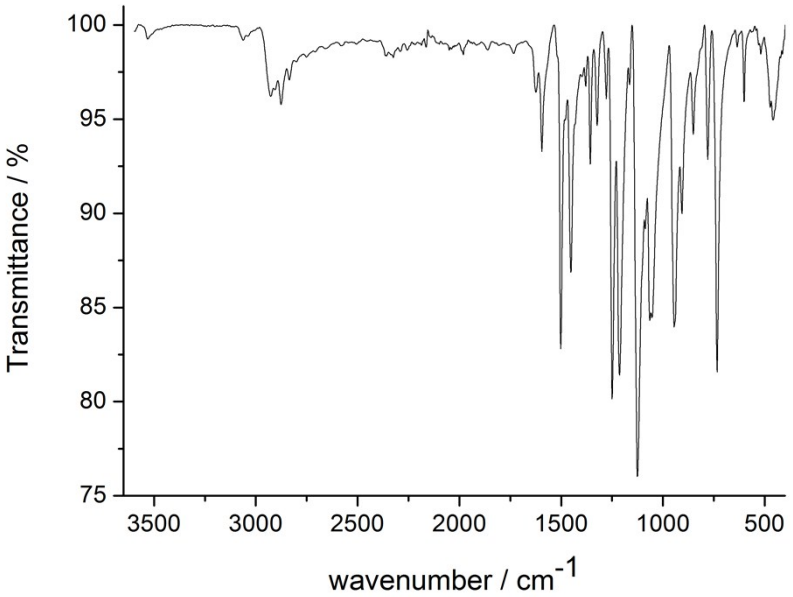

Figure S18. IR spectrum of compound **2**

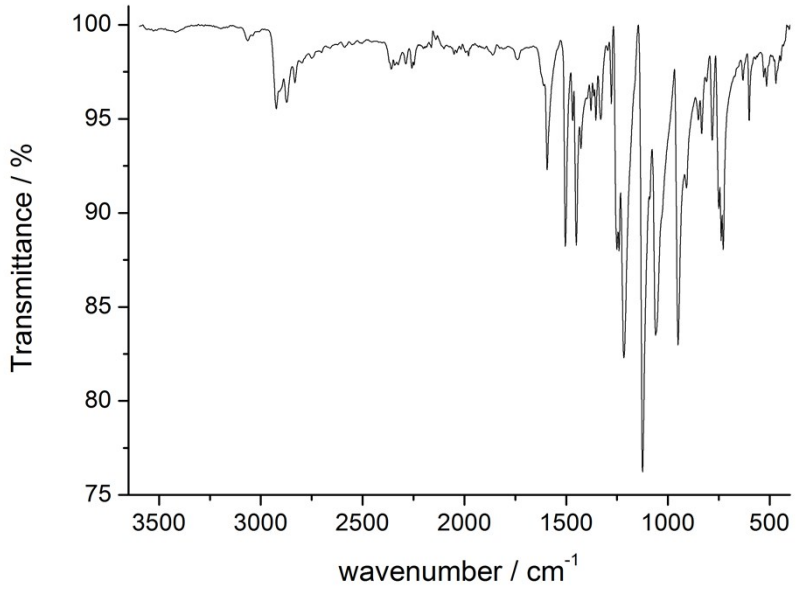

Figure S19. IR spectrum of compound **3**

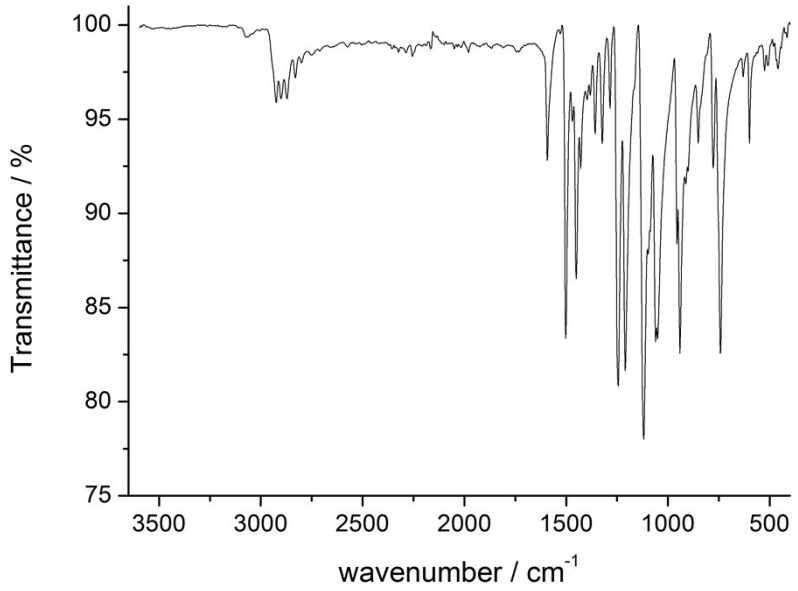

Figure S20. IR spectrum of compound **4**

Optical properties of the desolvated compounds

Optical absorption spectra were recorded on a *Varian Cary 5000* UV/Vis/NIR spectrometer in the range of 800-200 nm in diffuse reflectance mode employing a Praying Mantis accessory (*Harrick*). To assure that measurements were performed on the solvated compounds, single crystals of **1-4** were taken fresh from the mother liquor, freed from any adhering liquid on a filter paper, gently crushed into a powder between the filter paper and rapidly brought into the UV-VIS beam. Measurements on were also performed on the same samples after desolvation by drying at 170°C under vacuum for 1 h. Photographs shown as insets were taken after gentle desolvation by heating under an inert atmosphere.

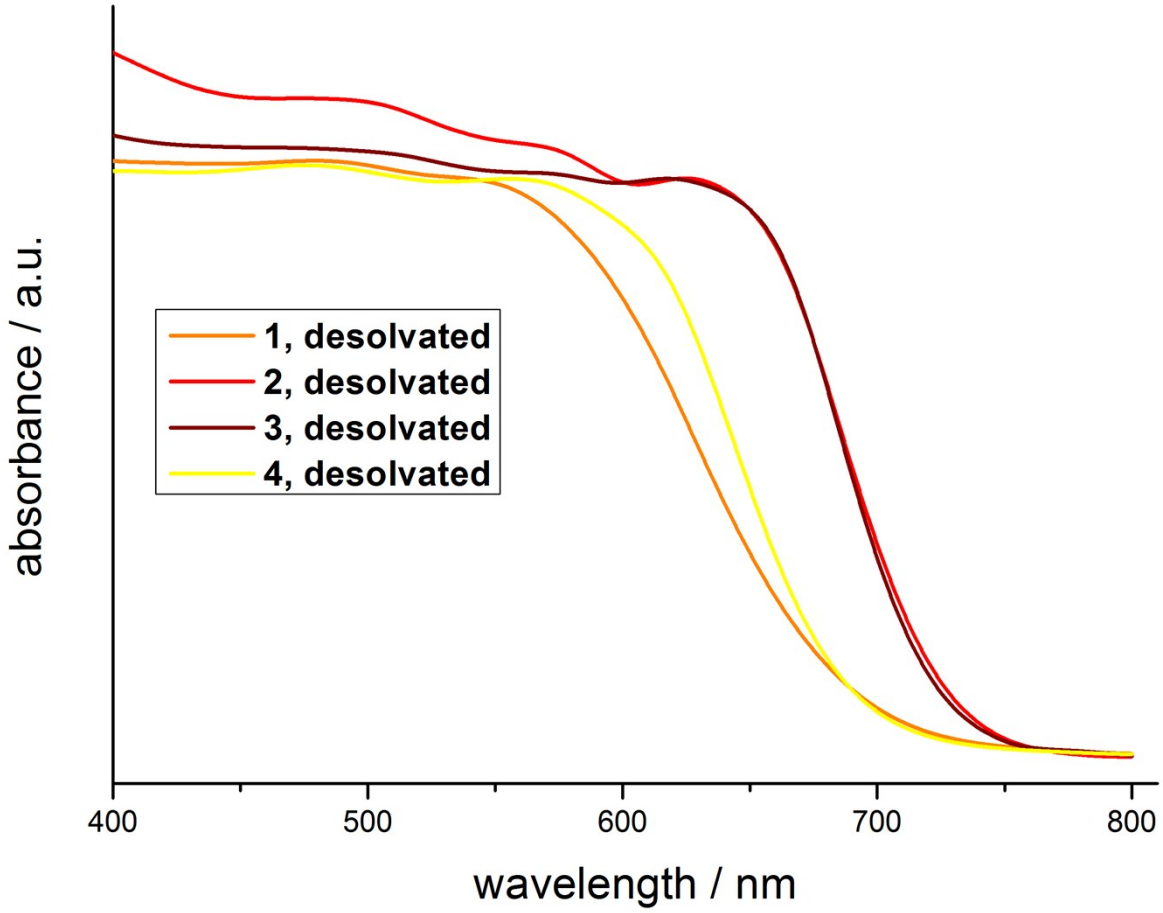

Figure S21. UV-Vis-spectra of the desolvated compounds

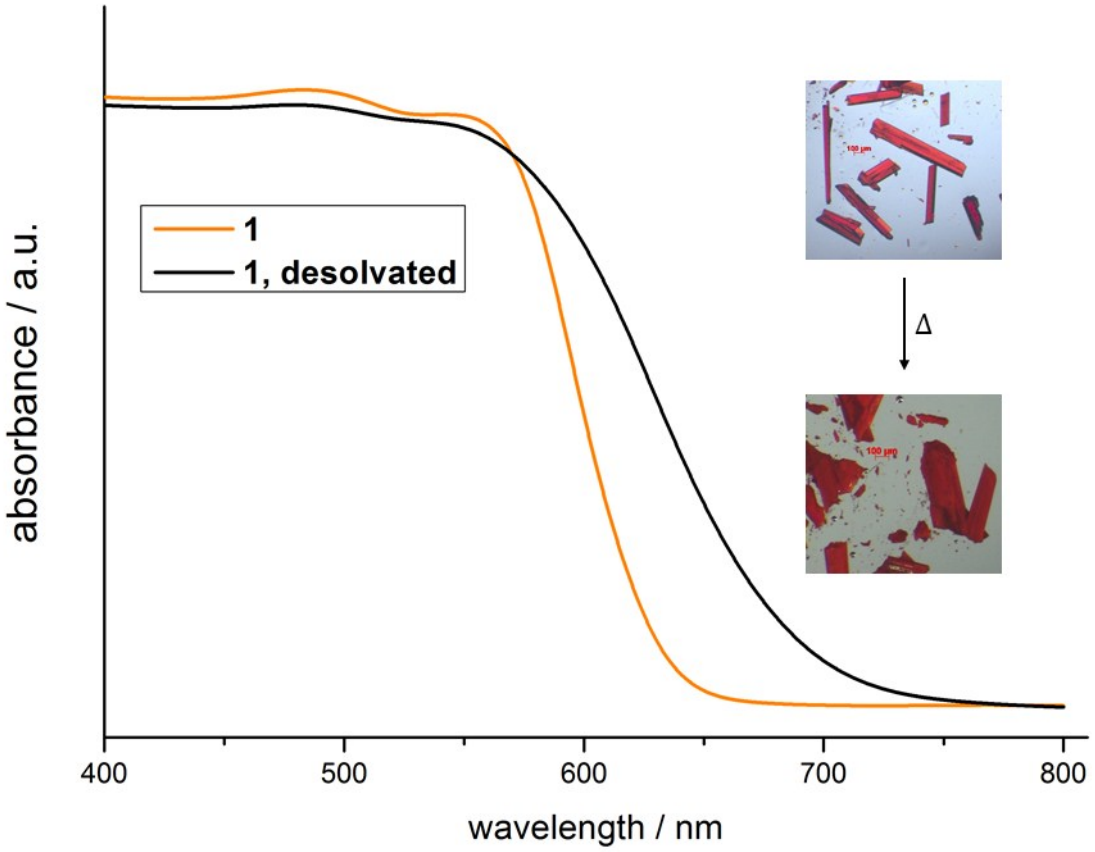

Figure S22. UV-Vis-spectra of **1** and desolvated **1**, with crystals before and after desolvation shown as an inset

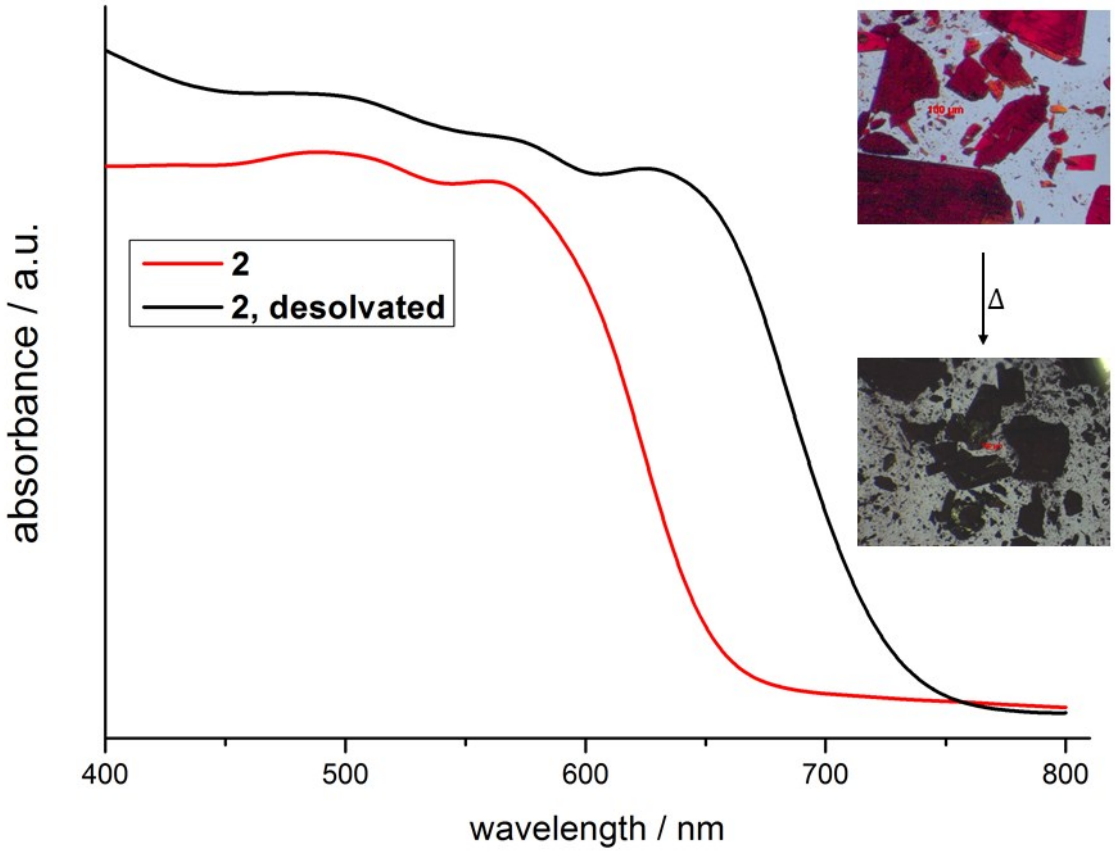

Figure S23. UV-Vis-spectra of **2** and desolvated **2**, with crystals before and after desolvation shown as an inset

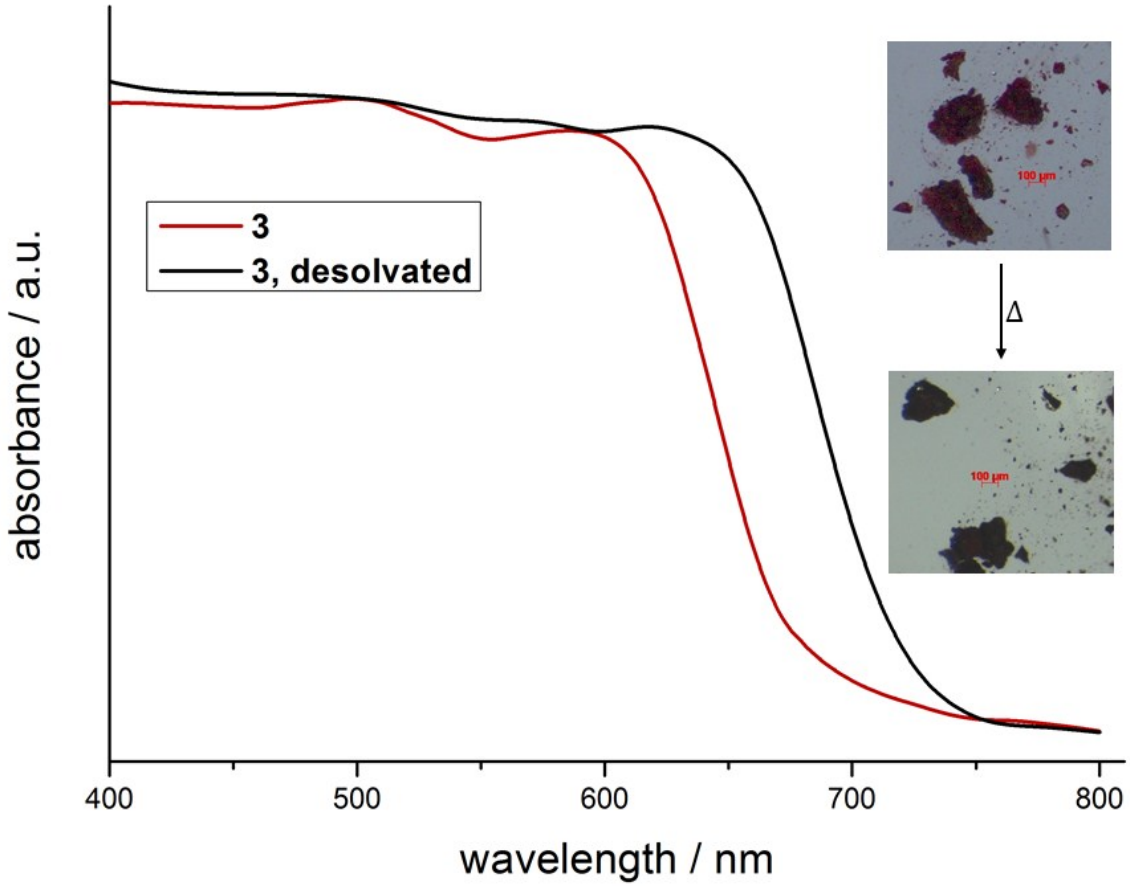

Figure S25. UV-Vis-spectra of **3** and desolvated **3**, with crystals before and after desolvation shown as an inset

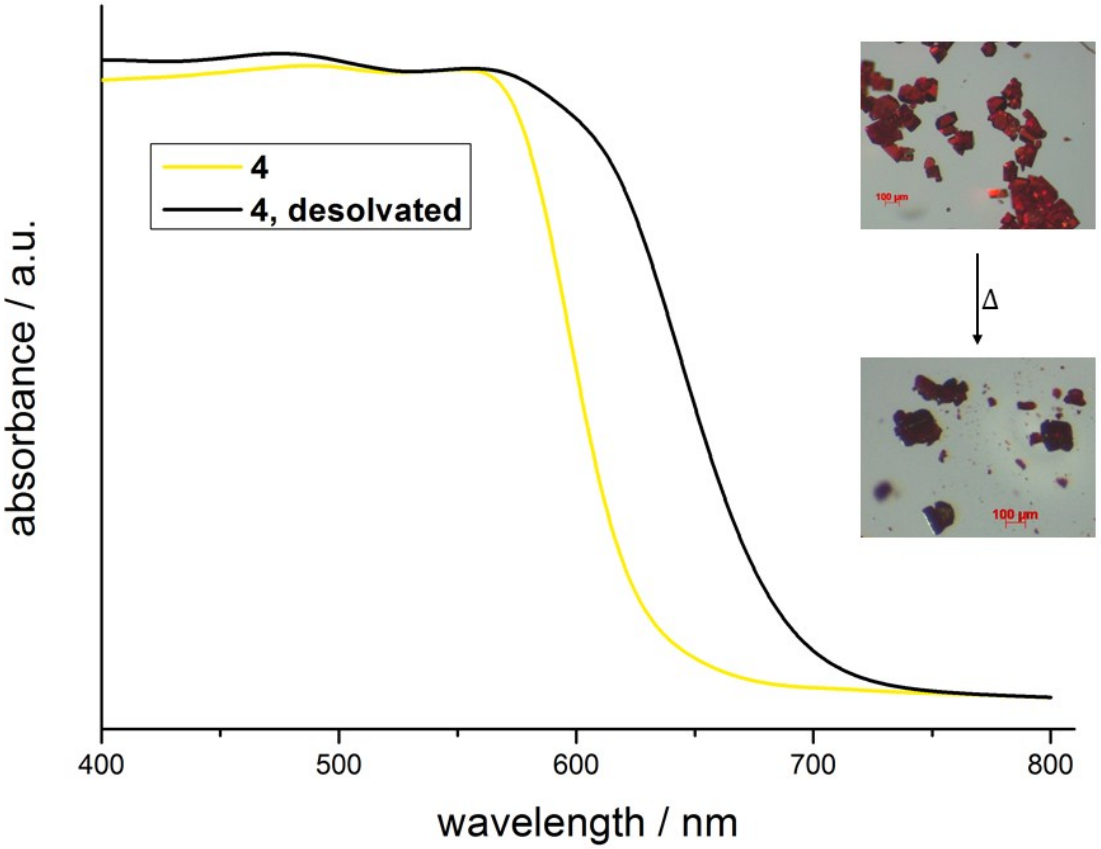

Figure S26. UV-Vis-spectra of **4** and desolvated **4**, with crystals before and after desolvation shown as an inset